Journal of Advances in Engineering Sciences and Technology, 2025, 1(1), 1-12
https://doi.org/10.71204/79qdc290

Research on Branch Traffic Flow Inversion and Monitoring Based on Main Road Data

Shuneng Lin [1,*]

[1] Shanghai Polytechnic University, Shanghai 201209, China

*** Correspondence**:

Shuneng Lin

1477793103@qq.com

Received: 14 May 2025/ Accepted: 18 June 2025/ Published online: 27 June 2025

Abstract

Accurate deduction of the historical trend of road branch traffic flow can provide data and method support for road resource planning and other issues. This paper proposes a branch traffic flow inversion and monitoring method based on main road data. Firstly, this study focuses on the typical Y-shaped road structure, and analyzes the single-peak variation characteristics of the traffic flow of branch 1 rising linearly with time and branch 2 rising first and then falling. The linear function and piecewise linear function are used to construct the sum relationship model of the traffic flow of the two branches and the main road. Then, the nonlinear least squares fitting is implemented by introducing the sequential least squares programming (SLSQP) algorithm, and reasonable boundary conditions and trend constraints are set. Finally, experimental verification shows that this method achieves extremely high fitting accuracy, clearly restores the trend of branch flow, and effectively verifies the scientificity and engineering practicability of the research method.

Keywords: Y-Shaped Road Structure; Branch Traffic Flow; Sequential Least Squares Programming

1. Introduction

In the modern urban transportation system, the efficient operation of the road network depends on accurate traffic flow monitoring and analysis. At present, the main road is usually equipped with advanced traffic flow monitoring equipment, which can record traffic flow data in real time and accurately, and provide an important basis for traffic management. However, when multiple branches merge into the main road, due to factors such as construction cost and space constraints, some branches often do not install traffic flow monitoring equipment, resulting in missing traffic flow data of these branches (Jabbar et al., 2022; Njoku et al., 2023). In this case, how to effectively infer the traffic flow of each branch by combining the traffic flow data of the main road and the historical trend information of the branch traffic flow has become a key problem to be solved in the field of transportation. Accurate estimation of branch traffic flow is of great significance for optimizing the timing of traffic lights, alleviating traffic congestion and rationally planning road resources. Accurate branch traffic flow data can help traffic management departments to set signal lamp duration more scientifically, reduce vehicle waiting time and improve road traffic efficiency (Yuan & Li, 2021; Jiang et al., 2022; Jiang et al., 2023). It can help to identify the source of traffic congestion, take timely measures to ease traffic pressure; it can also provide data support for the construction, expansion and reconstruction of urban roads, and realize the rational planning and allocation of road resources (Iyer, 2021; Shan et al., 2024).

Significant research has addressed traffic-related challenges through diverse approaches. For instance, an intelligent driver model integrating position-dependent lighting expectations was developed to analyze daytime bottlenecks in expressway tunnels (Yu et al., 2023). Separately, Zhang et al. (2022) introduced the GTA framework, leveraging spatio-temporal correlations from multi-sensor data for traffic prediction. However, inverse analysis of branch traffic flow remains a critical challenge, as existing methods exhibit distinct limitations. Current mainstream approaches primarily fall into two categories:

Statistically-based decomposition models, such as the Bayesian inference frameworks proposed by Mostafi et al. (2021), which assume Gaussian distributions but struggle to capture complex nonlinear dynamics.

Data-driven techniques, exemplified by graph neural networks developed by Wen et al. (2022), which improve accuracy but require multi-source sensor support and often neglect physical constraints, leading to unphysical solutions.

Recent advancements further highlight these gaps. Airaldi et al. (2025) proposed a highway ramp metering method integrating reinforcement learning and model predictive control, yet their approach relies on historical data for training and exhibits high computational complexity. Similarly, Lu et al. (2023) incorporated traffic flow theory constraints into neural networks for state estimation, though their applicability to Y-shaped topologies remains unvalidated. Chen et al. (2024) demonstrated network-level imputation potential using matrix/tensor completion techniques, but these methods notably fail to capture branch-specific unimodal patterns when relying solely on mainline data.

To bridge these critical gaps in modeling unimodal branch flows within Y-shaped networks—where existing approaches hard to capture characteristic single-peak patterns (Mostafi et al., 2021; Wen et al., 2022), neglect physical constraints (Airaldi et al., 2025; Lu et al., 2023), and lack topology-specific adaptability (Chen et al., 2024; Zhao et al., 2019)—this work introduces three key innovations:

A differentiated flow modeling paradigm that combines linear and piecewise-linear functions to explicitly address the distinct temporal dynamics of branch flows.

An enhanced SLSQP optimization framework embedding non-negativity, continuity, and endpoint constraints to ensure physical feasibility and computational efficiency.

A topology-specific inversion model designed for Y-shaped road networks, enabling precise urban traffic bottleneck analysis through reverse branch flow inference without reliance on historical branch data or multi-sensor infrastructure.

By integrating these innovations, the proposed method addresses the limitations of prior approaches, achieving superior accuracy and computational efficiency for branch traffic flow inversion tasks.

2. Establishment of Nonlinear Optimization Model

In the urban traffic network, the Y-type road network structure (two branches into a single main road) is highly typical. In this paper, the research scenario is shown in Figure 1, where the main road 3 is equipped with real-time monitoring equipment, which can obtain the traffic flow data in the morning rush hour, while the branch 1 and branch 2 lack direct observation means. Through the trend analysis of historical data, it is found that the traffic flow of branch 1 shows a strict linear growth law, while that of branch 2 shows a non-monotonic change characteristic of rising first and then falling, and its ' growth-falling ' process needs to be described by a piecewise linear function. This kind of differentiated flow evolution model puts forward special requirements for the construction of accurate branch flow inversion model.

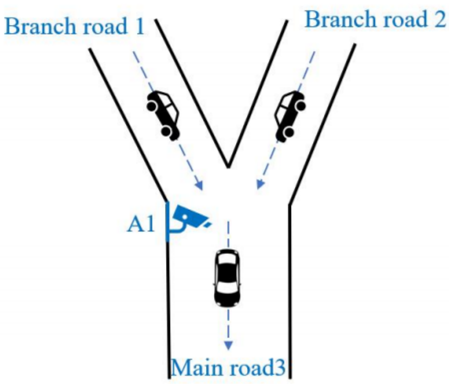

Figure 1. Road schematic

2.1. Variable Definition

The original time period is discretized into 60 time points at equal intervals, $t \in \{0,1,\ldots,59\}$, where $t = 0$ denotes 7: 00, and the corresponding actual time is increased by 2 minutes per step. Set the relevant traffic flow variables as:

- $f_1(t)$ represents the traffic flow of branch 1;
- $f_2(t)$ represents the traffic flow of branch 2;
- $F_3(t)$ denotes the actual observed traffic flow of main road 3 at time t;
- $F_{pred}(t)$ represents the traffic flow of the main road predicted by the model;

Here, $f_i(t)$ represents the traffic flow on the i^{th} branch road, while $F(t)$ denotes the traffic flow on the main road.

2.2. Branch Model Construction

We assume that the traffic flow of branch 1 shows a linear growth trend in the time period, indicating that the increase of traffic flow per unit time is constant, that is, the slope is fixed, which conforms to the typical first-order linear function characteristics.

Therefore, we set

$$f_1(t) = a_1 t + b_1 \tag{1}$$

where t represents the time point, a_1 represents the growth rate (slope) of traffic flow per unit time, and b_1 represents the initial traffic flow at $t = 0$ (i.e., 7: 00). Since the traffic flow should not be reduced, the slope should be positive, so there is a constraint $a_1 > 0$. The initial flow cannot be negative, so $b_1 \geq 0$.

Branch 2 shows a trend of "linear growth first and then linear decrease" during this period, that is:

- In the early stage, traffic flow increases with time;
- After reaching a certain peak (inflection point), the traffic flow begins to fall back.

This is a typical piecewise linear function structure, which can be concatenated by two linear functions with different slopes at a turning point t_p. We assume that:

$$f_2(t) = \begin{cases} a_{21} t + b_{21}, t \leq t_p \\ a_{22} t + b_{22}, t > t_p \end{cases} \tag{2}$$

where $a_{21} > 0$ represents the positive slope of the front segment; $a_{22} < 0$ indicates the negative slope of the posterior segment; $t_p \in (0,59)$ represents the peak time point of branch flow; b_{21}, b_{22} are the intercepts of the front and back function respectively.

Continuity requirements: the function must be continuous at $t = t_p$, and there can be no "jump" or "breakpoint". Therefore, it needs to meet:

$$a_{21} t_p + b_{21} = a_{22} t_p + b_{22} \tag{3}$$

The traffic flow of the road should be the sum of the traffic flow of the two roads at the same time point, that is:

$$F_{pred}(t) = f_1(t) + f_2(t) \tag{4}$$

$F_{pred}(t)$ is the predicted value of the main road flow in this paper. The goal is to make the predicted sequence as close as possible to the real observation data $F_3(t)$ of the main road.

2.3. Objective Function

In this paper, the least squares method is used to fit the parameters, that is, to construct an objective function of "residual sum of squares (SSR)":

$$SSR = \sum_{t=0}^{59} \left(F_{pred}(t) - F_3(t)\right)^2 \tag{5}$$

The objective function reflects the bias between the model's predicted value and the actual observed value, and the squared treatment avoids the cancellation of positive and negative residuals and a larger penalty on moments with larger deviations.

In order to enhance the physical reasonableness of the model, a penalty term is added to the objective function to control issues as negative values of the function, trend errors, and unreasonable end points. The final form of the optimization problem is:

$$\min_{t}\left[SSR(t)+\sum_{i}\lambda_{i}\cdot Penalty_{i}\right] \tag{6}$$

where λ_i is the weight of different penalty terms, $Penalty_i$ is the i^{th} penalty term, and the penalty term can be a soft constraint (embedded objective function).

2.4. Constraints

In order to ensure that the model conforms to the actual characteristics of traffic flow and avoid the "reasonable" solution in mathematical structure but "unreasonable" solution in practice, we need to clearly set multiple constraints:

(1) Parameter boundary constraints

$a_1 > 0$: the flow of branch 1 should rise with time; $b_1 \geq 0$: initial flow is non-negative; $a_{21} > 0$: the slope of the growth section of branch 2 is positive; $b_{21} \geq 0$: the initial flow of branch 2 is non-negative; $a_{22} < 0$: the slope of the descending section of branch 2 should be negative; $0 < t_p < 59$: the inflection point is located inside the interval to avoid boundary singularity.

(2) Non-negative constraint of function

In order to make the traffic flow of the model not negative at any time point, it is necessary to ensure that for all t:

$$f_1(t) \geq 0, f_2(t) \geq 0, F_{pred}(t) \geq 0 \tag{7}$$

Since the function structure itself is linear, the inappropriate selection of parameters may cause the appearance of local negative values. Therefore, during the optimization process, non-neg constraints are implemented through the penalty term:

$$Penalty_{neg}=\sum_{t}max\big(0,-f_1(t)\big)^2+max\big(0,-f_2(t)\big)^2+max\big(0,-F_{pred}(t)\big)^2 \tag{8}$$

Or if necessary, the key nodes are strongly constrained by inequality constraints.

(3) Inflection point continuity constraint

The piecewise linear function of branch 2 must be continuous at the inflection point t_p, otherwise there will be a "jump" phenomenon, which is not physically valid. Therefore, it is forced by the following equation:

$$b_{22}=(a_{21}-a_{22})t_p+b_{21} \tag{9}$$

This condition is not an explicit constraint in modeling, but is used to directly calculate b_{22} and simplify the optimization dimension.

(4) Terminal rationality constraint

At the last time point $t = 59$, the flow of branch 2 must also be non-negative, otherwise there will be a "sudden return to zero" or "backflow" problem. Therefore set:

$$f_2(59)=a_{22}\cdot 59+b_{22} \geq 0 \tag{10}$$

2.5. Overall Model

After synthesis, the model can be obtained as follows:

$$\min_{t}\left[\sum_{t=0}^{59}\left(F_{pred}(t)-F_3(t)\right)^2+\sum_{i}\lambda_i\cdot Penalty_i\right]$$

$$s.t.\begin{cases} a_1>0, b_1\geq 0, a_{21}>0, b_{21}\geq 0, a_{22}<0, 0<t_p<59 \\ f_1(t)\geq 0, f_2(t)\geq 0, F_{pred}(t)\geq 0 \\ Penalty_{neg}=\sum_t max\left(0,-f_1(t)\right)^2+max\left(0,-f_2(t)\right)^2+max\left(0,-F_{pred}(t)\right)^2 \\ b_{22}=(a_{21}-a_{22})t_p+b_{21} \\ f_2(59)=a_{22}\cdot 59+b_{22}\geq 0 \\ f_1(t)=a_1t+b_1 \\ f_2(t)=\begin{cases} a_{21}t+b_{21}, t\leq t_p \\ a_{22}t+b_{22}, t>t_p \end{cases} \end{cases} \tag{11}$$

In addition, the vector of all parameters to be optimized, denoted θ, is given by $\theta=[a_1,b_1,a_{21},b_{21},a_{22},t_p]$. Note that b_{22} is computed from the continuity constraint (Equation 9) and is not included directly as an independent optimization variable θ.

3. SLSQP Algorithm Solving Process

The model constructed in this paper is essentially a parameter optimization problem with nonlinear objective function and multiple constraints. Specifically, we hope that by adjusting the parameters of the branch traffic flow function, the predicted traffic flow of the main road can be as close as possible to the observed value. At the same time, the branch traffic flow is required to maintain non-negative, continuous function, reasonable trend and meet the boundary conditions at a specific time point. This series of constraints include both parameter boundaries and complex nonlinear inequality constraints.

Since the objective function is the sum of residual squares, its form is continuous and derivable, but it is not analytically solvable, so it needs to be solved by numerical optimization method. Among many numerical optimization algorithms, SLSQP algorithm has significant advantages. It is an algorithm based on the idea of sequential quadratic programming, which can simultaneously deal with continuous optimization problems with boundary constraints, equality and inequality nonlinear constraints. Compared with the traditional gradient descent or conjugate gradient method, SLSQP is more suitable for solving the optimization problems with smooth objective function, complex constraint structure and relatively small variable dimension.

In each iteration, the algorithm solves a quadratic programming sub-problem by constructing an approximate quadratic objective function and linearized constraints, so as to obtain the current optimal direction, and combines the line search mechanism to update the parameters until convergence. Based on these characteristics, SLSQP can not only efficiently deal with the complex constraints in the model, but also ensure that a stable optimal solution can be obtained within a reasonable calculation time. Therefore, we choose this algorithm as the main solution tool of this model. The following are the specific steps:

Step 1: construct the parameter vector. All the unknowns in the flow function of branch 1 and branch 2, such as slope, intercept, turning point position, etc., are sorted into a parameter vector as the decision variables of the optimization problem.

Step 2: Set the objective function. The sum of squared residuals between the predicted flow of the main road and the actual observed value is used as the objective function to reflect the fitting accuracy of the model. The better the fitting, the smaller the value of the objective function.

Step 3: Set constraints. The range of constraint parameters is introduced to ensure that the branch flow is non-negative, the trend direction is reasonable, the piecewise function is continuous, and the flow at the end of branch 2 is not negative, so as to enhance the physical rationality of the model.

Step 4: Call the SLSQP algorithm. Solve the nonlinear constrained optimization problem. The algorithm constructs a local quadratic approximation and linearizes the constraints at each iteration to calculate the update direction.

Step 5: Perform iterative update. The algorithm continuously optimizes the parameters through iteration, reduces the fitting error, and finally obtains the optimal parameter solution until the convergence condition is satisfied.

Step 6: Output the result function. Substituting the optimal parameters into the branch flow function, the traffic flow change model of branch 1 and branch 2 in the whole time period is obtained, and the traffic flow from the main road to the branch is reversed. The algorithm flow of this paper is shown in Algorithm 1.

Algorithm 1: SLSQP for Solving Branch Traffic Flow Model Parameters

Input: Main road observation data $F_3(t)$, time series $t = 0,1,\ldots,59$, model structures $f_1(t), f_2(t)$.

Output: Optimal parameter vector $\theta^* = [a_1, b_1, a_{21}, b_{21}, a_{22}, t_p]$.

1 Initialize the initial guess parameter θ_0;

2 Construct the objective function $SSR(\theta) = \sum_t (f_1(t) + f_2(t) - F_3(t))^2 + \text{Penalty Terms}$;

3 Set parameter constraints:

$\cdot\, a_1 > 0, b_1 \geq 0, a_{21} > 0, b_{21} \geq 0, a_{22} < 0$

$\cdot\, 0 < t_p < 59$

$\cdot\, f_2(59) \geq 0$

for $k = 1$ **to** maximum number of iterations **do**

Calculate the gradient $\nabla SSR(\theta_k)$ and the Jacobian matrix of the constraints;

Construct and solve the quadratic programming (QP) sub-problem to obtain the search direction d_k;

Line search to determine the step size α_k;

Update the parameter $\theta_{k+1} = \theta_k + \alpha_k d_k$;

if the convergence condition is met **then**

break

end for

return the optimal solution $\theta^* = \theta_k$

4. Model Solution Results and Analysis

4.1. Data Description

The data utilized in this study originates from the publicly released dataset of the 2025 China "May Day" Mathematical Modeling (Organizing Committee of May Day Mathematical Modeling Competition, 2025). Collected at a Y-shaped viaduct ramp, it comprises observed main road traffic flow values during the morning rush hour (7:00 to 8:58) on a specific weekday, sampled at 2-minute intervals, totaling 60 time points. Historical traffic flow analysis indicates distinct patterns within this period: Branch 1 exhibits sustained linear growth, whereas Branch 2 demonstrates a piecewise linear pattern characterized by initial growth followed by subsequent decline.

4.2. Experimental Analysis

The function expression obtained by solving is shown in Table 1:

Table 1. Branch traffic flow function expression

Branch 1	**Branch 2**
$f_1(t) = 0.2571t + 1.5989$	$f_2(t) = \begin{cases} 1.2394t + 6.0087, 0 \le t \le 30 \\ -0.7288t + 64.5973, t > 30 \end{cases}$

In order to better analyze the fitting effect of the model, we also introduce R^2 score to determine the fitting effect of the model. The R^2 score is an indicator of the goodness of fit of the regression model, reflecting the proportion of data variability explained by the model, and it is also the final criterion for us to determine which model to choose. The calculation formula is:

$$R^2 = 1 - \frac{\sum_{i=1}^{n} (\hat{y}_i - y_i)^2}{\sum_{i=1}^{n} (y_i - \bar{y})^2} \tag{12}$$

where y_i is the true value, $\hat{y}_i$ is the predicted value, and $\bar{y}_i$ is the average value of y_i.

By solving, we get the minimum SR of the model is 7.02, and the R^2 score is 0.9841. In order to better show the fitting effect, the following visualization is shown in Fig.2.

According to the comparison between the fitted curve and the observed data in the Fig.1, we make the following analysis and conclusions on the model fitting effect and the trend of branch traffic flow:

The red dotted line represents the traffic flow of branch 1, which shows a linear upward trend as a whole, reflecting the continuous growth of traffic flow in branch 1 during the morning peak period, and the rate of vehicles entering the main road per unit time remains stable, which is in line with the typical morning peak commuting characteristics. This trend also verifies the rationality of the assumption of 1 "linear growth" of branches in the proposition.

The blue dotted line represents the traffic flow of branch 2, which rises rapidly in the first half, and begins to decline after reaching the peak at about $t = 29.77$ (corresponding to about 8: 00), forming a typical single-peak structure. It shows that the traffic flow carried by branch 2 is mainly concentrated in the early morning peak, and the traffic flow drops significantly after the peak. The change trend is consistent with the actual traffic law of the "short-term concentration" branch during the morning peak period.

The total traffic flow of the main road (green solid line) predicted by the model is highly consistent with the actual observation data (black dots). The two basically overlap in the whole period of time, and there is only a small local deviation, indicating that the established branch traffic flow function and the main road prediction structure can effectively capture the real traffic behavior, and the fitting error is well controlled.

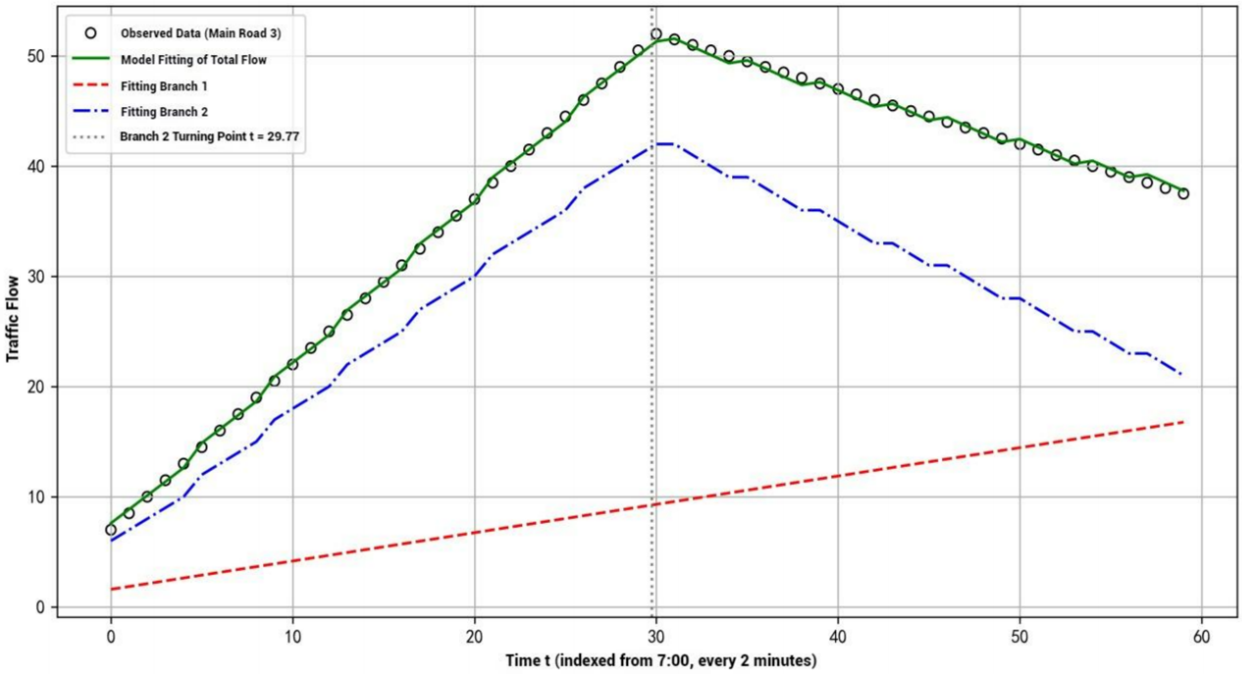

Figure 2. Visual fitting diagram

4.3. Comparison of method performance

To validate the superiority of the proposed method, we compare its performance against the Bayesian linear regression model (Mostafi et al., 2021), Bayesian multivariate linear regression model (Mostafi et al., 2021), and the graph convolutional network (GCN) model (Wen et al., 2022) on the same dataset.

https://doi.org/10.71204/79qdc290

As summarized in Table II, the results demonstrate that: the simple Bayesian linear regression model achieves a relatively low R^2 of 0.5244 due to its neglect of the unilateral characteristics of traffic flow, while the Bayesian multivariate linear regression model improves this to 0.9589 but requires 0.3226 seconds of computation. The graph convolutional network (GCN) further enhances the R^2 to 0.9756, yet it demands multi-branch historical data and incurs a significantly higher computational cost of 4.6836 seconds. In contrast, the proposed method achieves the highest accuracy of R^2 = 0.9841 with a guaranteed zero negative flow constraint and an exceptionally low computational cost of only 0.0212 seconds, outperforming all benchmarks in both precision and efficiency. This highlights the proposed framework's ability to balance high accuracy, physical feasibility, and computational scalability for branch traffic flow inversion tasks.

Table 2. Comparison of inversion method performance

Method	R2	Calculation time (s)
Bayesian linear regression	0.5244	0.0017
Bayesian Multivariate Linear Regression	0.9589	0.3226
Graph convolutional network	0.9756	4.6836
Method in this paper	0.9841	0.0212

5. Conclusion

With the close connection between intelligent transportation and urban planning, the rational planning of road resources is very important to alleviate traffic congestion and improve travel efficiency. The accurate deduction of the historical trend of road branch traffic flow can undoubtedly provide a solid data cornerstone and effective method support for this key field.

Based on this background, this paper innovatively proposes a branch traffic flow inversion framework based on main road data, addressing key limitations in existing approaches. The framework introduces a piecewise linear constrained optimization model to capture the "first increase, then decrease" dynamics of unimodal flows, incorporating Sequential Least Squares Programming (SLSQP) with physical constraints (non-negativity, continuity) to ensure both accuracy and feasibility. A Y-shaped topology-specific inversion model is established to overcome the poor adaptability of generalized models, eliminating dependencies on historical branch data and reducing deployment costs compared to multi-sensor-based schemes. Experimental validation demonstrates that the proposed method achieves high fitting accuracy and robust performance, providing cost-effective solutions for traffic signal optimization and bottleneck identification.

However, the current model assumes piecewise linear dynamics, which may limit its applicability to complex nonlinear patterns. Future work will explore B-spline basis functions and genetic algorithm-based optimization to construct a universal nonlinear inversion model, validate the framework using multi-source data, and extend it to multi-branch networks via hierarchical constraint modeling. These advancements target enhanced scalability, accuracy, and practicality in large-scale urban systems, ultimately bridging the gap between theoretical innovation and real-world implementation.

Funding:

This research received no external funding.

Institutional Review Board Statement:

Not applicable.

Data Availability Statement:

These data were derived from the following resources available in the public domain: https://51mcm.cumt.edu.cn/63/bc/c14143a680892/page.htm.

Acknowledgments:

I thank my friends and family for their patience during the long hours devoted to this self-directed project. While every aspect this work was independently executed, their emotional support helped sustain my motivation. Any limitations or errors in this paper remain my sole responsibility

Conflict of Interest:

The authors declare no conflict of interest.

References

Airaldi, F., De Schutter, B., & Dabiri, A. (2025). Reinforcement learning with model predictive control for highway ramp metering. IEEE Transactions on Intelligent Transportation Systems, 26(5), 5988-6004.

Chen, P., Li, F., Wei, D., et al. (2024). Spatiotemporal traffic data completion with truncated minimax-concave penalty. Transportation Research Part C: Emerging Technologies, 164, 104657.

Iyer, L. S. (2021). AI enabled applications towards intelligent transportation. Transportation Engineering, 5, 100083.

Jabbar, R., Dhib, E., Said, A. B., et al. (2022). Blockchain technology for intelligent transportation systems: A systematic literature review. IEEE Access, 10, 20995-21031.

Jiang, P., Fan, Z., Pan, M., et al. (2022). Research of traffic flow saturation on waters of the coastal ship routing system. Ocean Engineering, 263, 112417.

Jiang, Y., Ren, T., Ma, Y., et al. (2023). Traffic safety evaluation of mixed traffic flow considering the maximum platoon size of connected automated vehicles. Physica A: Statistical Mechanics and its Applications, 612, 128452.

Lu, J., Li, C., Wu, X. B., et al. (2023). Physics-informed neural networks for integrated traffic state and queue profile estimation: A differentiable programming approach on layered computational graphs. Transportation Research Part C: Emerging Technologies, 153, 104224.

Mostafi, S., Alghamdi, T., & Elgazzar, K. (2021). A Bayesian linear regression approach to predict traffic congestion. In 2021 IEEE 7th World Forum on Internet of Things (WF-IoT) (pp. 716-722). IEEE.

Njoku, J. N., Nwakanma, C. I., Amaizu, G. C., et al. (2023). Prospects and challenges of Metaverse application in data - driven intelligent transportation systems. IET Intelligent Transport Systems, 17(1), 1-21.

Organizing Committee of May Day Mathematical Modeling Competition. (2025). Dataset for 2025-51MCM-Problem A. https://51mcm.cumt.edu.cn/63/bc/c14143a680892/page.htm

Shan, Y., Xie, X., Sun, J., et al. (2024). Resilient design of networked security control for active suspension systems via an augmented switching-type approach. IEEE/ASME Transactions on Mechatronics. (In press)

Wenjuan, X., & Jianfeng, L. (2022). Research on traffic flow forecasting method based on graph neural network. In 2022 IEEE 2nd International Conference on Software Engineering and Artificial Intelligence (SEAI) (pp. 243-247). IEEE.

Yu, S., Zhao, C., Song, L., et al. (2023). Understanding traffic bottlenecks of long freeway tunnels based on a novel location-dependent lighting-related car-following model. Tunnelling and Underground Space Technology, 136, 105098.

Yuan, H., & Li, G. (2021). A survey of traffic prediction: From spatio-temporal data to intelligent transportation. Data Science and Engineering, 6(1), 63-85.

Zhang, C., James, J. Q., & Liu, Y. (2019). Spatial-temporal graph attention networks: A deep learning approach for traffic forecasting. IEEE Access, 7, 166246-166256.

Zhao, Z., Wang, Z., Wu, G., et al. (2019). The state-of-the-art of coordinated ramp control with mixed traffic conditions. In 2019 IEEE Intelligent Transportation Systems Conference (ITSC) (pp. 1741-1748). IEEE.